Journal of Biomechanics 49 (2016) 580–585

Contents lists available at ScienceDirect

Journal of Biomechanics

journal homepage: www.elsevier.com/locate/jbiomech
www.JBiomech.com

A stricter condition for standing balance after unexpected perturbations

At L. Hof [a,b,*], Carolin Curtze [b,c]

[a] Centre for Human Movement Sciences, University of Groningen, The Netherlands
[b] Centre for Rehabilitation, University Medical Centre Groningen, The Netherlands
[c] Department of Neurology, School of Medicine, Oregon Health & Science University, Portland, OR, USA

ARTICLE INFO

Article history:
Accepted 28 January 2016

Keywords:
Balance
Equilibrium
Base of support
Centre of mass
Centre of pressure
XcoM
CoP
CoM

ABSTRACT

In order to account for the dynamic nature of balance, the concept of the 'extrapolated centre of mass' XcoM has been introduced (Hof et al., 2005). The law for standing balance was then formulated as: the XcoM should remain within the Base of Support (BoS). This law, however, does not take into account that the centre of pressure (CoP) needs time to displace due to various neural and mechanical delays.

The theory is extended to include the finite reaction- and displacement time of the CoP. Experimental results on humans standing on two feet undergoing sudden postural perturbations are presented. In this case it turns out that the area of the effective BoS is only a fraction, some 30%, of the area of the static BoS.

1. Introduction

The classical formulation for balance has been put as: the vertical projection of the centre of mass (CoM) should be within the base of support (BoS). In order to account for the dynamic nature of balance stability in a standing person or an animal, we have introduced the concept of the 'extrapolated centre of mass' XcoM (Hof et al., 2005). In this concept, the XcoM is defined as the velocity-adjusted CoM position. The balance law then becomes: the XcoM must remain within the boundaries of the BoS. The concept XcoM has proved useful in several applications, e.g. Bierbaum et al. (2011), Curtze et al. (2011), and MacLellan and Patla (2006). In our 2005 paper the traditional concept of BoS was adopted unchanged: the BoS is the area in which the CoP can possibly be located. This definition assumes that the CoP can change position infinitely fast. While this may be a viable assumption for rigid objects, like tables and chairs, in living beings the CoP can only be displaced by muscle action. This needs finite time, the neuronal delay followed by a gradual build-up of muscle force. In the 2005 paper the issue was adressed, by reference to time-to-contact methods, but not solved. Later developments of the theory now make a solution possible.

* Correspondence to: Centre for Human Movement Sciences, University of Groningen, PO Box 196, 9700 AD Groningen, The Netherlands. Tel.: +31 50 403 1773.
E-mail address: a.l.hof@umcg.nl (A.L. Hof).

http://dx.doi.org/10.1016/j.jbiomech.2016.01.021
0021-9290/

1.1. Theory

The theory is based on the inverted pendulum model of (human) balance, of which the planar version is shown in Fig. 1. The weight mg of the body can be thought concentrated in the CoM, with horizontal coordinate x. This weight is counteracted by a ground reaction force of the same magnitude but opposite direction and positioned at the CoP with coordinate u. The CoP is located within the BoS, with boundaries u_{min} and u_{max}. When the excursions of x are small compared to the leg length, one can derive from the equations of motion a second order differential equation in x (Hof, 2008b).

$$\frac{d^2x}{dt^2} = \omega_0^2(x-u) \tag{1}$$

in which $\omega_0 = \sqrt{\frac{g}{l}}$, with g the acceleration of gravity and l the 'effective pendulum length', 1.24 or 1.34 times leg length (Hof et al., 2005). By introducing a new variable, the 'extrapolated centre of mass (XcoM)' $\xi = x + \frac{1}{\omega_0}\frac{dx}{dt}$ the second-order differential equation (1) can be written as two coupled fist-order differential equations (Hof, 2008b):

$$\frac{d\xi}{dt} = \omega_0(\xi - u) \tag{2}$$

$$\frac{dx}{dt} = -\omega_0(x-\xi) \tag{3}$$

The inverted pendulum model (1), which predicts CoM position $x(t)$ from a given CoP trajectory $u(t)$ can thus be presented as a cascade of two subsystems (Fig. 2), relation (2) which gives $\xi(t)$ as a function of $u(t)$ and relation (3), which gives $x(t)$ from $\xi(t)$. An alternative derivation of (1)–(3) with the Laplace transform can be found in the Appendix.

The important difference between Eqs. (2) and (3) is that the subsystem described by Eq. (3), with the minus sign, is stable, while the first subsystem (2) is unstable (Hof, 2008b). From this it follows that it is sufficient to control subsystem (2). For standing this implies that to keep balance, the XcoM $\xi(t)$ should be kept within the BoS. (In this view it is the most logical to locate the XcoM at ground level, like the BoS, while the CoM is at some height.)

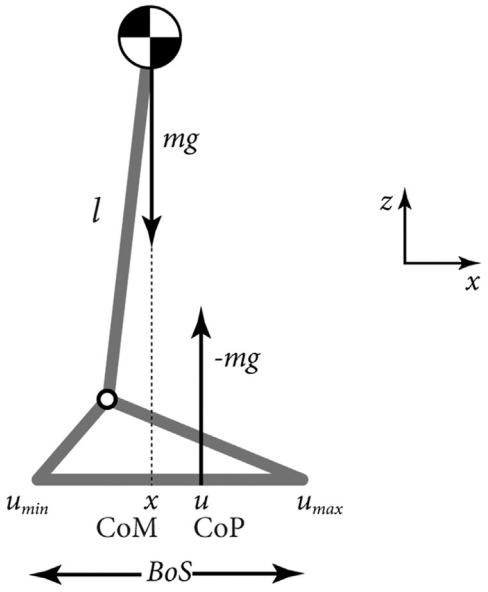

Fig. 1. Schematic diagram of the inverted pendulum model. The body is modelled as a single mass balancing on top of a stick with length l. Indicated are the location of the Centre of Pressure (CoP) u, the location of the effective ground reaction force, and the vertical projection of the Centre of Mass (CoM) x. The Base of Support (BoS) is the area to which the CoP is confined.

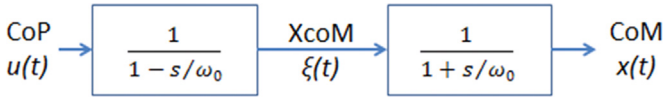

Fig. 2. The inverted pendulum model, as a cascade of two subsystems, left according to Eq. (2), right according to Eq. (3). The subsystems are indicated by their frequency-domain transfer functions (A4) and (A5) respectively.

The problem to be answered in this paper is to find the conditions for the position of the XcoM ξ_0 after an unexpected postural perturbation, such that $\xi(t)$ will remain within the BoS when the CoP displacement $u(t)$ is not infinitely fast. In principle this is straightforward: solve the differential Eq. (2) for a time varying $u(t)$ and see if the resulting XcoM $\xi(t)$ will remain within the BoS. In principle this would entail solving the unstable differential Eq. (2) several times with various initial conditions ξ_0 to iterate to a solution of $\xi(t)$ that just ends at u_{max}, the boundary of the BoS. In practice this can be done simpler by solving the differential equation backwards from t_e, the time $u(t)$ reaches the boundary of the BoS, down to $t=0$, thus by adopting a new time scale $t'=(t_e-t)$. In that case the differential equation becomes

$$\frac{d\xi}{dt'}=\frac{d\xi}{d(t_e-t)}=-\omega_0(\xi-u(t')) \tag{4}$$

Using this trick, we now get a stable differential equation, of the form of (3), which can be solved by filtering the reversed $u(t')$ by a first order filter with cut-off frequency ω_0 and initial condition $\xi'(t_e)=u_{max}$. Filtering backward until $t=0$ (or $t'=t_e$) we will find $\xi'(0)$ the maximal value of ξ that can lead to stable balance. It will be clear that we have to discriminate between the static BoS, the area in which the CoP can possibly be located, and the effective BoS 'eBoS', the area in which the initial XcoM should be located so that balance can be restored.

The purpose of the present paper is to present experimental data on $u(t)$, the time course of the CoP after a sudden perturbation, and to discuss the consequences for the effective base of support in human two-legged standing.

In the experiments it was as a rule not possible for $u(t)$ to exactly arrive at u_{max}, the boundary of the BoS. Instead we have calculated a 'reduction coefficient' r, i.e. the fraction

$$r=\frac{\xi'(0)-u(0)}{u(t_{peak})-u(0)} \tag{5}$$

in which $u(t_{peak})$ is the peak value of $u(t)$ in the experiment, and have assumed that the same ratio can be used for $u(t_{peak})=u_{\max}$.

Table 1
Personal data for the subjects. Reduction coefficient r for forward, backward, leftward and rightward perturbations, median values of 3–4 measurements. There were significant differences between subjects (Kruskal–Wallis test, $p<0.005$) but not between conditions.

Subject	Age (yr)	Mass (kg)	Stature (m)	Leg length (m)	r Forward	r Backward	r Right	r Left
1	49	81.0	1.89	1.04	0.5278	0.6520	0.5109	0.5359
2	64	101.0	1.92	1.01	0.5487	0.5760	0.5772	0.5771
3	47	73.5	1.81	0.99	0.5778	0.5527	0.5190	0.5565
4	68	101.5	1.97	1.05	0.5440	0.5150	0.5129	0.4807
5	52	82.0	1.79	0.92	0.4557	0.5637	0.5175	0.5183
6	63	96.5	1.94	1.03	0.5384	0.5473	0.5925	0.5684
7	56	70.5	1.79	1.00	0.6538	0.5722	0.5677	0.5749
8	41	92.5	1.80	0.94	0.4395	0.3711	0.4781	0.4464
9	46	99.0	1.91	1.00	0.5232	0.5688	0.5457	0.5692
10	44	89.0	1.85	0.93	0.4361	0.5009	0.5715	0.5326
11	62	79.5	1.86	0.96	0.5167	n.a.	0.5618	0.5370
Mean					0.5245	0.5511	0.5387	0.5369
Std					0.0665	0.0628	0.0404	0.0445
n					34	33	36	38

2. Methods

2.1. Subjects, equipment

The 11 experimental subjects were taken from the control group of an earlier study (Curtze et al., 2013). They were healthy males with ages between 41 and 68 yr (Table 1). Ground reaction forces were measured by two AMTI force plates sampled at 1000 Hz. Kinematics was tracked by an eight camera Vicon motion capture system at a rate of 100 Hz. A total of 35 reflective markers were placed as specified in the Vicon Plug-in-Gait full-body model. The toe and heel markers were used to specify the location of both feet, the complete set of marker data were input to the Plug-in-Gait model for calculating the whole body CoM. The subjects had their shoes on. The toe marker was placed over the second metatarsal head at the break of forefoot and toes, the heel marker at the hindmost position on the heel of the shoe. From the CoM coordinates the XcoM coordinates were calculated according to the definition in the Introduction. For the differentiation a first order finite difference method was used.

The perturbation was applied by means of a horizontal cable from the subject's waist to a pulley (Fig. 3). A weight hung at the end of the cable, connected by an electromagnet. The force in the cable was measured by a force transducer.

2.2. Procedure

The subject stood upright with his feet parallel, each foot on a separate force plate. While standing the subject resisted the load, which was at an unexpected moment released by the experimenter. This induced a fall opposite to the pulling direction. The falls were induced in four directions: forward, backward, right and left. The order of perturbations was randomized over participants, at least three trials were performed per direction. Measurements in which the CoP action $u(t)$ was not maximally fast, visible in the derivative of the $u(t)$ curve, were excluded. This was done in 12 cases, so that 141 valid measurements remained.

The load was set to 2.5% of body weight for forward/backward perturbations and 5% of body weight for left/right perturbations. The distance between the medial edges of the feet was set to 20% of waist height. The participants were instructed to resist the perturbation without making a step. They were secured with a safety harness from the ceiling. The study was approved by the local Medical Ethical Committee.

2.3. Data analysis

The moment of release ($t=0$) was determined from the signal of the cable force transducer. The CoP under each foot was determined by standard methods from signals of the two separate force plates, and the common CoP signal $u(t)$ as the weighted mean of left and right CoP (Winter, 1995b). CoP signals were filtered forward-backward with a 50 Hz second order Butterworth filter. CoM and XcoM were calculated from the kinematic data. In the Vicon Plug-in-Gait model the kinematic data are filtered by a zero-lag filter with a cut-off at 4–6 Hz (Woltring, 1985). This filtering is different from the 50 Hz filter for the CoP, which will be accounted for in the interpretation of the results. The initial values of CoP and XcoM, u_0 and ξ_0 were calculated as the averages of u and ξ over the interval from -1 to -0.5 s before the release. In this way, the erroneous values of ξ due to the filtering were excluded. Coordinates are expressed in mm relative to the Vicon coordinate origin, with x left/right and y backward/forward.

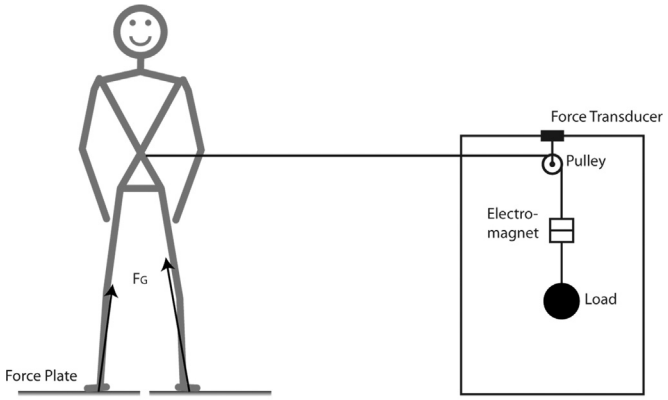

Fig. 3. Experimental set-up. The subject resists a pulling force, from the left in this figure. This force ends abruptly when the electromagnet is released. This force release is read from the force transducer. The subject stands with two feet each on a separate force plate.

The CoM derived from kinematic data included a systematic error that needed to be removed. Assuming that the average position of the CoM and the CoP needs to be the same during quiet standing, the averages were substracted from each other over the last second, when the subject has returned to quiet standing. This difference was added to the CoM coordinates.

The 'maximum XcoM' $\hat{\xi}$' was calculated from $u(t)$ by selecting the first peak in $u(t)$ after $t=0$. The part of $u(t)$ between $t=0$ and $t=t_{peak}$ was then reversed and filtered by a first order (Butterworth) filter with cut-off ω_0 and intitial condition $\xi'(t_{peak})=u(t_{peak})$. The final value $\xi'(0)$ served as the outcome and was expressed as the 'reduction coefficient' r according to (5).

To determine group effects a Kruskal–Wallis test was done. A non-parametric test was used because of the small number of measurements 3–4 per subject and per condition.

3. Results

Fig. 4A shows a recording of a backward fall, after release from a forward pull, for a typical subject. Before the release average CoP is at 174 mm and the CoM and XcoM at 217 mm. The difference of 43 mm is because of the horizontal force. After the release at $t=0$, the XcoM immediately starts to increase. The CoP shows a delay of about 120 ms, then rises steeply from 174 to 260 mm at $t=395$ ms. As soon as the CoP passes the XcoM, the latter stars to decrease, cf. (2). More gradually and with a few oscillations the CoP returns to a a value around 190 mm. The CoM follows the XcoM with more delay and a lower amplitude; its initial value is 216 mm, with a peak of 229 mm at $t=632$ ms, so the CoM shifts no more than 13 mm thanks to the swift action of the CoP. In the final phase, when the subject has returned to quiet standing, CoP, XcoM and CoM come closely together.

The 'maximal XcoM' calculated from the peak of the CoP backward to $t=0$ equals 220 mm, which gives a $r=0.56$. In principle the measured XcoM should remain below this maximal curve. In the figure this is not exactly the case. This is an artefact due to the low-frequency (4–6 Hz) zero-lag filtering of the kinematic data, on which the CoM and the XcoM are based. The zero-lag property also makes that CoM and XcoM already seem to increase before the release, which is not realistic.

An x–y plot of the CoP and XcoM curves is shown in Fig. 4B. CoP and XcoM move in a fairly straight line backward and forward over the midline between the two feet. Because we recorded the ground reaction forces of both feet on separate force plates, we can show the CoP trajectories of both feet separately. Both run in a straight line over the feet, from the midpoint of the heel towards a point between the 2nd and 3rd toe.

The results for a forward fall, Fig. 5AB are closely identical to those for the backward fall. The difference is that the boundaries of the BoS are much further away. In this subject and condition the correction of the XcoM by the CoP involved three to-and-fro oscillations. The time course of the CoP resulted in a value of r close to that in the backward fall. The CoP trajectories of both feet (Fig. 5B) followed the same line as in Fig. 4, but now further forward.

Perturbations in the frontal plane, like the rightward fall in Fig. 6A, show a few differences with those in the for-aft direction. After the release there is an immediate increase in the CoP curve, with an inflection at 130 ms. The complete redress of the perturbation takes a shorter time, about 2 s, even if the initial perturbation was larger, 60 mm instead of 40 mm in Figs. 4 and 5. The left and right CoP trajectories (Fig. 6B) follow the same course as in Figs. 4 and 5, but over a shorter distance. The right–left CoP movement is brought about by changes in the right and left ground reaction forces, thus by the weight shifting strategy.

Data on the reduction coefficient r have been given in Table 1. The given data are median values of 3–4 measurements, the group averages are calculated from all available data. A Kruskall–Wallis

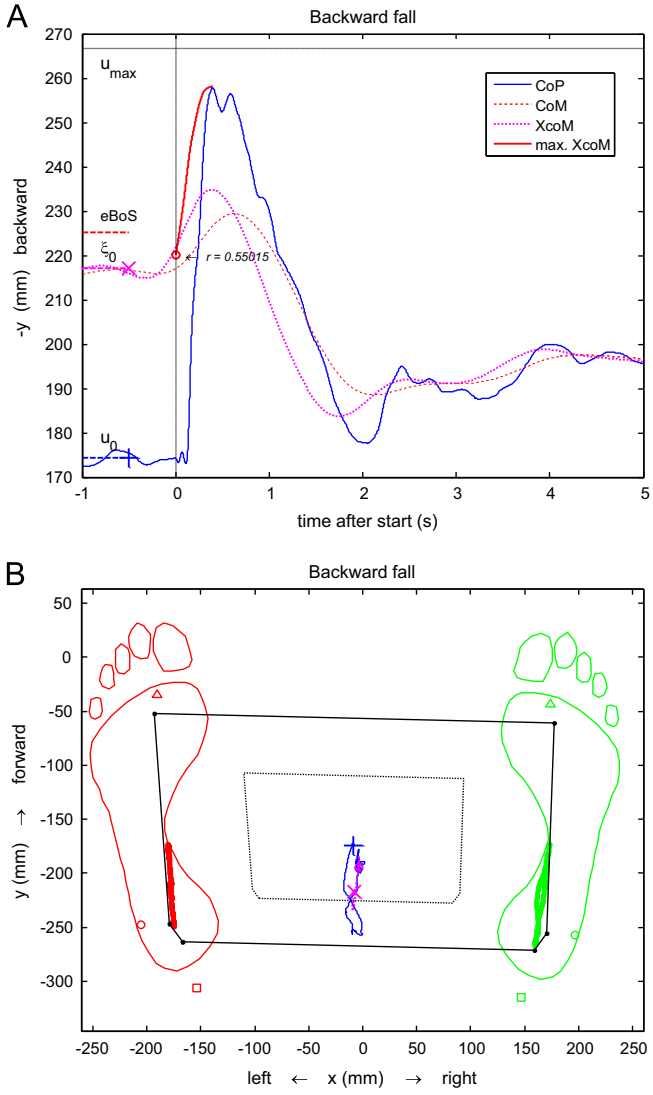

Fig. 4. Backward fall. A CoP (thin solid line), CoM (dotted) and XcoM (dashed) as a function of time. Release of the forward force is at $t=0$. Thick solid line: maximum XcoM as computed from the CoP, see Methods. At the left, from bottom to top, the pre-perturbation values of, CoP (+), XcoM (and CoM, '×') and the boundaries of eBoS and BoS (u_{max}, thin dotted line). B X–Y recording of CoP, CoM and XcoM. Both the common CoP (thin line) and the separate CoPs of left and right foot (thick lines) are shown. Foot outlines are based on the heel (□) and toe (Δ) markers. The outlines of the bare feet are shown, but the subjects wore shoes in the experiment. Further are shown: pre-perturbation values of, CoP (+), XcoM (and CoM, '×'), final values of CoP and CoM (O), ankle marker (o). Solid broken line: boundaries of BoS. Dotted line: boundaries of the eBoS. The vertices of the eBoS were determined as r times the distance from initial CoP (+) to the corresponding BoS vertices (.).

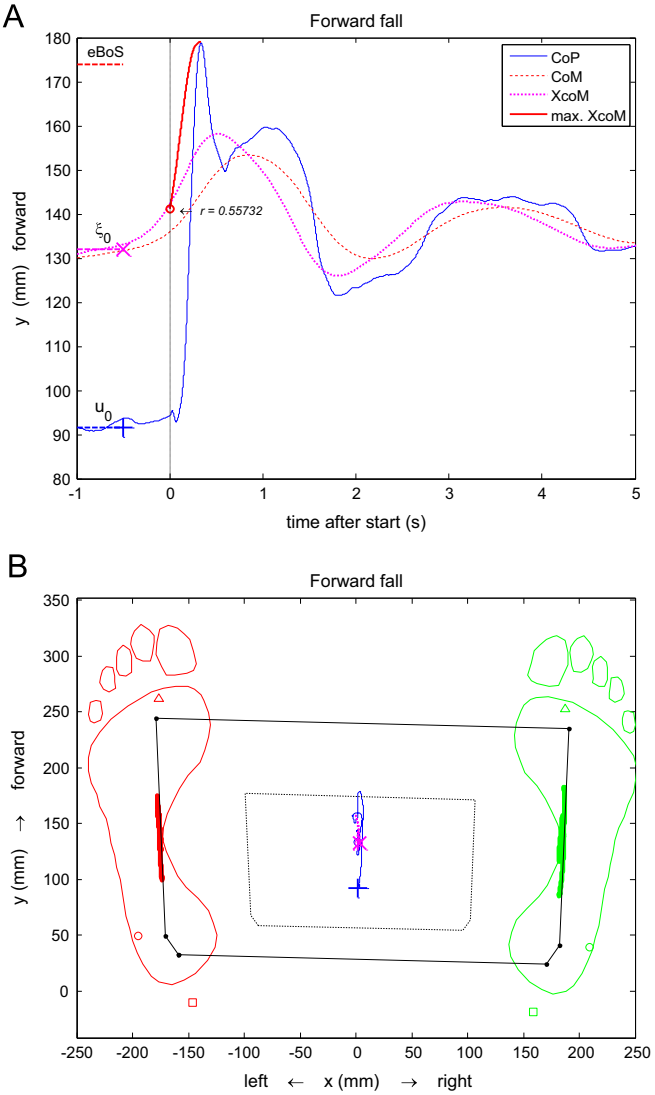

Fig. 5. Forward fall, see legend of Fig. 4. The forward boundary of the BoS was at 239 mm (not shown in Fig. 5A).

test showed no significant effect of fall condition, but a significant effect of the subject ($K=59$, $p<0.005$).

The findings on the trajectories of the left and right CoPs enable us to construct the BoS. The trajectory of the right foot in Fig. 4B suggest that the lower right vertex is situated at the middle of the heel. We have supposed that the upper right one is at the edge of the forefoot between the second and third toe, on the same straight line. The middle vertex is close to the heel, but more laterally. These three vertices can be constructed in the figures on the basis of the positions of the heel and toe markers. The left vertices of the BoS were assumed symmetrical. Together they allowed the BoS to be constucted in the three figures. Data to construct the BoS vertices from the kinematic data are given in Table 2. In all subjects the agreement with the measured left and right CoP trajectories was good.

When the reduction factor r is known from the CoP time course, the effective BoS, 'eBos' can be constructed, the dotted line in Figs. 4B, 5B, 6B. The eBoS is centred around the initial CoP position u_0 (+ in Figures), see Eq. (5). The vertices of the eBoS thus lie on lines between u_0 and each BoS vertex at a fraction of r of the distance from u_0.

It is seen that in the subject presented (subject 6 in Table 1) the CoP excursions come fairly close to the BoS in backward falls (Fig. 4B), but not in the other conditions.

4. Discussion

It is evident from the reported experiments that in standing the effective BoS is considerably smaller than the 'area between the feet' as commonly supposed. The reduction factor r (Table 1) is on average of the order of 0.54, with considerable interindividual differences. The 'eBoS' thus has an area only $(0.54)^2=0.3$ times the area of the static BoS. What this means in practice is illustrated in Fig. 4A and B. The initial value of the XcoM was 217 mm, the BoS is at 267 mm, one might thus conclude to an ample margin of 50 mm. In fact the eBoS was at 225 mm, the true margin of stability was thus only 8 mm.

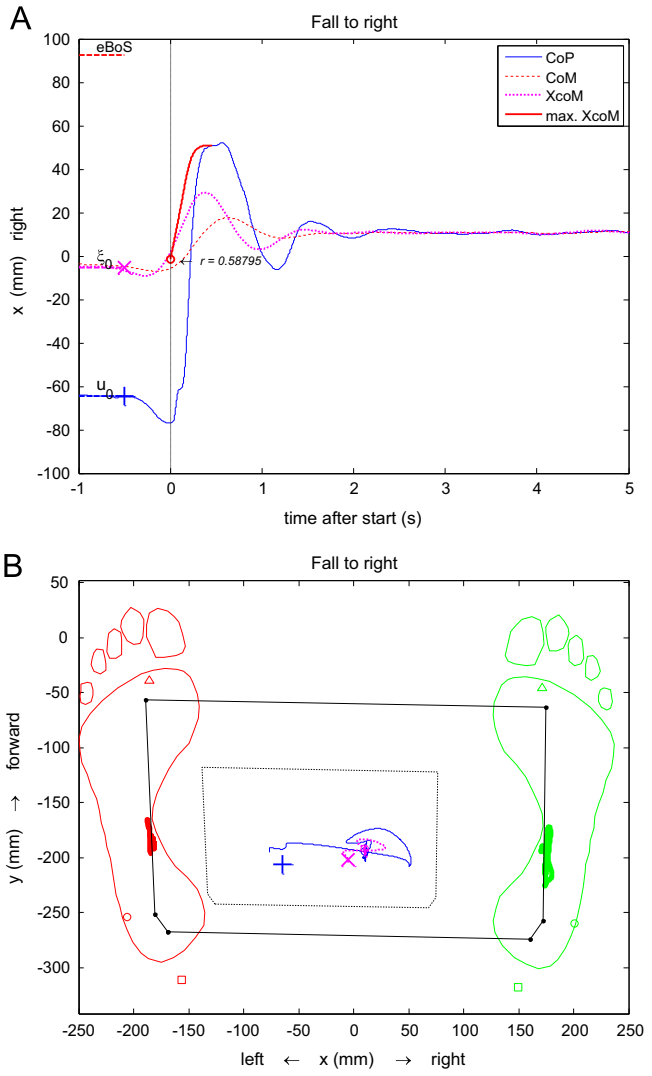

Fig. 6. Fall to the right, see legend of Fig. 4. The boundaries of eBoS (92 mm) and BoS (202 mm) fall outside the vertical scale of Fig. 6A.

Table 2
Position of vertices of the BoS for two-legged standing, given as a fraction of the heel-toe marker distance. (note that the toe-marker is at the MTP2 joint). The perpendicular distances for the right/left foot are all to the right/left, respectively.

Vertex	From heel	To right/left
1	0.162	0.027
2	0.225	0.063
3	0.937	0.018

The proportion between eBoS and BoS, the reduction factor r, depends on the time course of the CoP $u(t)$ after an initiated fall. This time course will depend on the balance strategy involved. In our two-legged standing experiment this is the sagittal ankle strategy for for-aft fals and the weight shifting strategy for left–right perturbations (Winter, 1995a; Hof, 2008a). Although different muscle groups are involved, ankle plantar/dorsiflexors and hip abductors, respectively, r-values were on the average not different (Table 1).

4.1. CoP reaction to perturbation

The CoP time course $u(t)$ for the fore-aft motion has been recorded in earlier experiments, e.g. (Henry et al., 1998; Küng et al., 2009). The response starts with a delay of 120–130 ms and is followed by a fast movement towards a peak at 300–600 ms. The lateral CoP movement seems to include a passive component of some 15 mm, which starts immediately at the release and is followed by the delayed muscle response (Fig. 6A).

One may expect that with other strategies r can be different. For the stepping strategy, typically a delay of 280 ms, followed by a CoP movement of 200 ms is given (Hsiao-Wecksler et al., 2003; Carty et al., 2011). This would result in r around 0.3, but with a larger BoS. By expressing the effect of finite time $u(t)$ in a single coefficient r according to Eq. (5) we have implicitly assumed that the value of r is independent of the amplitude of $u(t)$. This assumption needs further investigation, but there are some indications that it is indeed valid. The backward fall in Fig. 4 had a CoP excursion close to the boundary of the BoS. It thus gives a representative r-value for extreme balance perturbations. The forward and right falls, as in Figs. 5 and 6, had their XcoM well within the eBoS, but their r-values were on average the same.

4.2. Practical use

The theory in Eqs. (1)–(5) gives a neat division between the mechanical balance challenge, the perturbation $(\xi_0 - u_0)$ vs. the BoS distance $(u_{max} - u_0)$, and the individual response, expressed in the non-dimensional number r. Our results suggest significant interindividual differences in this coefficient. Provided that individual values of r can be determined sufficiently precise, it may be a sensible measure for individual balancing capacities in a certain strategy, the experiment is simple enough (Luchies et al., 1994; Hsiao-Wecksler et al., 2003; Curtze et al., 2013).

Even without taking temporal factors into account, defining the BoS requires some consideration. Much depends on the balance strategies allowed to the subject. In our experiments the subject had to remain standing and only the sagittal ankle strategy and the weight shifting strategy were allowed. Even then, we had to make an educated guess as to the forward boundary of the BoS. A more definitive determination would have required a series of perturbations of increasing size. If stepping had been allowed, the standing eBoS as presented here would have been surrounded by a wider eBoS for stepping. Similarly, if trunk or arm motion had been taken into account, the BoS and eBoS would have widened as well (Curtze et al., 2010).

4.3. A measure of stability?

In the first paragraph of this Discussion we used the distance between the XcoM and the boundary of the eBoS, as a measure of the 'margin of stability'. Thus

$$d_{margin} = u_0 + r(u_{max} - u_0) - \xi_0 \quad (6a)$$

Practice will show if such a margin is a sensible measure of stability. The conditions of the experiment and the related theory should be kept in mind in this respect: quiet standing on two feet, that is suddenly perturbed, so that a fall is initiated.

Several authors have used a related 'margin of stability', the instantaneous distance between XcoM and BoS (Bierbaum et al., 2011; Hak et al., 2013) as a measure for stability during a movement, e.g. walking. On the basis of the present theory it could thus be suggested to choose the instantaneous distance between the boundary of the eBoS and the XcoM instead. This would give:

$$d(t) = u(t) + r(u_{max} - u(t)) - \xi(t) \quad (6b)$$

In our opinion such a measure is not without problems. Most movements are not stable at all times, even in our force release experiment the XcoM goes temporarily outside of the eBoS, see Fig. 4, and even if the changing eBoS boundaries are accounted for

(according to Eq. 6b), there is a short time of instability, when the XcoM has started to move and the CoP has not yet sufficiently reacted. In walking the problem is even more complicated. Most of the time the balance is unstable, and the XcoM is outside of the BoS or eBoS of either stance foot (Hof, 2008b). For a practical measure of walking balance more theory seems needed.

Conflicts of interest

There are no conflicts of interest to report.

APPENDIX

Alternative derivation eqs. (2) and (3).

We write eq. (1) in the Laplace transform:

$$s^2X(s) = \omega_0^2(X(s)-U(s)) \tag{A1}$$

Where $X(s)$ and $U(s)$ are the Laplace transforms of $x(t)$ and $u(t)$, respectively. This gives the transfer function from $U(s)$ to $X(s)$:

$$X(s) = \frac{1}{1-\left(\frac{s}{\omega_0}\right)^2}.U(s) \tag{A2}$$

The polynomial in the denominator has two roots, $s = +\omega_0$ and $s = -\omega_0$, so that we can write

$$X(s) = \frac{1}{1-\left(\frac{s}{\omega_0}\right)}.\frac{1}{1+\left(\frac{s}{\omega_0}\right)}U(s) \tag{A3}$$

This can be interpreted as the concatenations of two first order transfer functions, with an – as yet unspecified- intermediate variable $\Xi(s)$, see Figure 2.

$$\Xi(s) = \frac{1}{1-\left(\frac{s}{\omega_0}\right)}.U(s) \tag{A4}$$

$$X(s) = \frac{1}{1+\left(\frac{s}{\omega_0}\right)}.\Xi(s) \tag{A5}$$

Back transforming (A4) and (A5) into the time-domain yields eqs. (2) and (3), respectively. A5 also defines the XcoM, as from (A5) follows

$$\Xi(s) = \left(1+\left(\frac{s}{\omega_0}\right)\right)X(s) \tag{A6}$$

In the time domain this means

$$\xi(t) = x(t) + \frac{1}{\omega_0}.\frac{dx}{dt} \tag{A7}$$

In this way the XcoM is derived from the inverse pendulum model (1) in a simpler way than originally in (Hof et al., 2005).

References

Bierbaum, S., Peper, A., Karamanidis, K., Arampatzis, A., 2011. Adaptive feedback potential in dynamic stability during disturbed walking in the elderly. J. Biomech. 44, 1921–1926.

Carty, C.P., Mills, P., Barrett, R., 2011. Recovery from forward loss of balance in young and older adults using the stepping strategy. Gait Posture 33, 261–267.

Curtze, C., Hof, A.L., Postema, K., Otten, B., 2011. Over rough and smooth: amputee gait on an irregular surface. Gait Posture 33, 292–296.

Curtze, C., Hof, A.L., Postema, K., Otten, B., 2013. The relative contributions of the prosthetic and sound limb to balance control in unilateral transtibial amputees. Gait Posture 36, 276–281.

Curtze, C., Postema, K., Akkermans, H.W., Otten, B., Hof, A.L., 2010. The Narrow Ridge Balance Test: a measure for one-leg lateral balance control. Gait Posture 32, 627–631.

Hak, L., Houdijk, H., Steenbrink, F., Mert, A., van der Wurff, P., Beek, P.J., van Dieën, J. H., 2013. Stepping strategies for regulating gait adaptability and stability. J. Biomech. 46, 905–911.

Henry, S.H., Fung, J., Horak, F.B., 1998. EMG responses to maintain stance during multidirectional surface translations. J. Neurophysiol. 80, 1939–1950.

Hof, A.L., 2008a. Mechanics of balance. In: D'Août, K., Lescrenier, K., van Gheluwe, B., De Clercq, D. (Eds.), Advances in Plantar Pressure Measurements in Clinical and Scientific Research. Shaker, Maastricht, pp. 1–25.

Hof, A.L., 2008b. The 'extrapolated center of mass' concept suggests a simple control of balance in walking. Hum. Mov. Sci. 27, 112–125.

Hof, A.L., Gazendam, M., Sinke, W.E., 2005. The condition for dynamic stability. J. Biomech. 38, 1–8.

Hsiao-Wecksler, E.T., Katdare, K., Matson, J., Liu, W., Lipsitz, L.A., Collins, J.J., 2003. Predicting the dynamic postural control response from quiet-stance behavior in elderly adults. J. Biomech. 36, 1327–1333.

Küng, U.M., Horlings, C.G., Honegger, F., Duysens, J., Allum, J.H., 2009. Control of roll and pitch motion during multi-directional balance perturbations. Exp. Brain Res. 194, 631–645.

Luchies, C., Alexander, N.B., Schultz, A.B., Ashton-Miller, J., 1994. Stepping responses of young and old adults to postural disturbances: Kinematics. J. Am. Geriatr. Soc. 42, 506–512.

MacLellan, M.J., Patla, A.E., 2006. Adaptations of walking pattern on a compliant surface to regulate dynamic stability. Exp. Brain Res. 173, 521–530.

Winter, D.A., 1995a. ABC of Balance During Standing and Walking. Waterloo Biomechanics, Waterloo, CA.

Winter, D.A., 1995b. Human balance and posture control during standing and walking. Gait Posture 3, 193–214.

Woltring, H.J., 1985. On optimal smoothing and derivative estimation from noisy displacement data in biomechanics. Hum. Mov. Sci. 4, 229–245.